AIAA JOURNAL
Vol. 39, No. 7, July 2001

Structural/Acoustic Sensitivity Analysis of a Structure Subjected to Stochastic Excitation

Michael J. Allen*
University of Michigan, Ann Arbor, Michigan 48109-2145
Ricardo Sbragio†
Cidade Universitária, 05508-900 São Paulo, Brazil
and
Nickolas Vlahopoulos‡
University of Michigan, Ann Arbor, Michigan 48109-2145

A development for computing the structural/acoustic sensitivity of systems subjected to stochastic excitation is presented. Previous work in the area of structural/acoustic sensitivity analysis considered systems subject to deterministic excitations. The sensitivity computation depends on the excitation; therefore, new algorithms are developed to account for stochastic excitation. The structural/acoustic sensitivity is calculated using finite element methods, boundary element methods, and stochastic analysis techniques. Structural/acoustic sensitivities for the radiated sound pressure spectral density and the radiated sound power are computed. The sensitivity values are calculated with respect to a set of sizing structural design variables. The random pressure distribution exerted on the surface of the structure by turbulent boundary-layer flow is considered as excitation. Two classic structural models, a simply supported plate and a stiffened simply supported plate, are analyzed to demonstrate and validate the algorithms. Structural/acoustic sensitivity results are compared successfully to data computed by finite difference analyses.

Nomenclature

$[A]$, $[B]$	=	acoustic boundary element method (BEM) system matrices
$\{A\}$, $\{B\}$	=	acoustic BEM system vectors
$[Ar]$	=	diagonal elemental area matrix
$[B]$	=	damping matrix
$E[\,]$	=	expected value
$\{F\}$	=	nodal forcing vector
H	=	transfer function
i	=	$\sqrt{-1}$ imaginary number
$[K]$	=	stiffness matrix
$[M]$	=	mass matrix
PW	=	radiated acoustic power
$\{p\}$	=	nodal acoustic pressure
$Q(\omega)$	=	acoustic response quantity
$\{R\}$	=	response vector
$S(\omega)$	=	spectral density
$[T]$	=	transformation matrix
$\{u\}$	=	nodal displacement vector
$\{v\}$	=	nodal velocity vector
Δ	=	change in structural design variable
$\partial/\partial h$	=	sensitivity with respect to design variable h
ω	=	radian frequency

Superscripts

H	=	Hermitian transpose
$*$	=	complex conjugate

Introduction

THE analysis of structural/acoustic systems and how changes in their design variables impact the radiated noise is an ongoing and evolving area of active research. Finite element methods (FEM)[1,2] and boundary element methods (BEM)[3–7] are the two main numerical techniques utilized for computing the response of structural/acoustic systems. In uncoupled simulations, a harmonic excitation is applied on the structure and the vibration is computed (FEM). Then, the structural vibration is used as the excitation for the acoustic analysis (FEM or BEM). Thus, the noise generated from the vibration of a structure is computed.

Several current analysis techniques employ FEM and BEM for calculating the sensitivity of the acoustic response with respect to a structural design variable.[8–13] FEM are utilized for computing the vibratory response and the dependency of the vibration to the structural design variables (structural sensitivities). The vibration of the structure constitutes the excitation for the acoustic computations. The acoustic response, the acoustic sensitivity, the structural vibration, and the structural sensitivity are utilized in the computation of the combined structural/acoustic sensitivity. The overall acoustic response is typically represented in terms of radiated acoustic pressure or radiated sound power, and therefore, the sensitivities represent the anticipated change in these quantities with respect to a structural design variable. The structural/acoustic sensitivity computation depends on the excitation applied on the structure. Existing sensitivity formulations consider only a deterministic excitation.

In several industries (aerospace, automotive, and naval), operating structures are subjected to stochastic excitation produced by the boundary layer that is generated from an external flow. In aerospace applications, the boundary layer of the external airflow applies a fluctuating pressure on the fuselage and noise is transmitted in the interior.[14–16] In automotive applications, efforts are pursued for reducing interior wind noise generated from the airflow around the vehicle.[3,17,18] Noise transmitted through the side glass window system is a particular concern.[18,19] In the naval industry, the boundary-layer excitation can induce vibrations on the hull of a vessel and generate noise.[20]

In this paper, structural/acoustic sensitivity algorithms are presented for systems that are subjected to stochastic excitation. The effect of structural design variables on the radiated acoustic pressure and the radiated sound power is computed. The algorithms that determine the sensitivity of the sound pressure spectral density and the sound power are derived from principles of stochastic analysis, finite element analysis, and boundary element analysis. The sensitivity algorithms provide means for assessing the

Received 3 July 2000; revision received 15 January 2001; accepted for publication 24 January 2001.

*Graduate Research Assistant, Department of Naval Architecture and Marine Engineering; currently Assistant Professor, Department of Aerospace and Ocean Engineering, Virginia Polytechnic Institute and State University, Blacksburg, VA 24061.

†Head, Naval Engineering Division, Navy Technological Center, São Paulo, Av. Professor Lineu Prestes 2242.

‡Associate Professor, Department of Naval Architecture and Marine Engineering, 2600 Draper Road. Member AIAA.

impact of changes in the structural/acoustic behavior of systems subjected to stochastic excitation. The fluctuating pressure associated with turbulent boundary-layer airflow is considered as the stochastic excitation applied on the structure. Boundary-layer excitation is well documented.[21–25] Experimental data and a boundary-layer model available from the literature[24,25] are employed for defining the stochastic excitation in this paper. However, the algorithms that compute the structural/acoustic sensitivity are general, and any stochastic excitation that can be defined by auto- and cross-spectral density terms may be utilized in the sensitivity computations. Two structures with simple geometry and a moderate number of degrees of freedom are analyzed. The first structure is a simply supported plate subjected to boundary-layer excitation from one side and radiating noise in a free field from the opposite side. The second structure is a stiffened simply supported plate created by adding two transverse L-shaped stiffeners placed equidistant along the length of the original simply supported panel. Similar models have been used in previous research regarding noise transmission, acoustic sensitivity, and noise transmission associated with turbulent boundary layers.[23,25–29] Sensitivity values are calculated for the two structural panels that are analyzed. The sensitivities are utilized to predict the changes that will occur in the sound pressure spectral density and the radiated sound power when a set of structural design variables is perturbed. The predicted changes in the acoustic response are compared to changes in the sound pressure spectral density and the sound power values obtained through finite difference analysis. Good correlation is observed between the sensitivity and the finite difference results. The work presented in this paper contributes significant tools to the field of noise and vibration analysis. New algorithms are formulated, implemented, and validated for computing the following: 1) radiated acoustic power for systems subjected to stochastic excitation, 2) structural/acoustic sensitivity of the autospectral density of the radiated acoustic pressure, and 3) structural/acoustic sensitivity of the radiated sound power.

Theory

In this section, the formulation that computes the noise radiated from a structural/acoustic system subjected to stochastic excitation[26,30] is reviewed. The autospectral density of the radiated acoustic pressure is computed by combining the spectral definition of the random excitation with a set of transfer functions between pressure excitation applied on the structure[26] and the radiated noise. The transfer functions are computed by FEM and BEM. The transfer functions are combined with the auto- and cross-spectral densities of the excitation to produce the spectral density of the radiated acoustic pressure. An algorithm for computing the radiated power for a system subjected to stochastic excitation is presented. The transfer functions between excitation and acoustic surface pressure are combined with the transfer functions of the surface velocity, the structural surface area, and the stochastic excitation to produce the radiated sound power.

Sensitivity algorithms are developed by differentiating the formulas that calculate the acoustic spectral density, and the radiated power, with respect to structural design variables. The transfer functions that associate structural vibration with the stochastic excitation are differentiated, and the structural sensitivity is computed. The structural sensitivity captures the dependency of the structural vibration to the design variables when the structure is subjected to stochastic excitation. The transfer functions that associate either the spectral density of the acoustic pressure or the radiated power to the structural vibration are differentiated for computing the acoustic sensitivity. The acoustic sensitivity identifies the dependency of the acoustic pressure and the acoustic power to the structural vibration that has been generated from a stochastic excitation. The structural and the acoustic sensitivities are combined to compute the structural/acoustic sensitivity. The latter identifies how the level of the radiated noise or the radiated power depends on structural design variables for systems that are subjected to stochastic excitation.

Radiated Acoustic Pressure Spectral Density

The calculation of the spectral density of the radiated acoustic pressure is based on combining a set of transfer functions, associated with the structural/acoustic system, with the spectrum of the random excitation.[26,30] The transfer functions represent a relationship between a unit uniform excitation placed over a section of the structure and the acoustic pressure response at locations of interest within the acoustic medium. The area where the random excitation is applied is divided into a set of panels. A unit excitation is applied on each panel, and transfer functions between panel excitation and acoustic response at the field points are calculated. Criteria based on convergence of the solution have been developed for determining the proper panel subdivision.[26]

The FEM is used to calculate the vibration of the structure when the excitation is applied over each panel. The structural vibration constitutes the boundary condition in a boundary element analysis that computes the radiated noise at every data recovery point of interest. The finite element system of equations for a multidimensional vibrating structure subject to a harmonic excitation can be expressed in matrix form as follows[31]:

$$[St]\{u\} = \{F\} \tag{1}$$

where $[St] = -\omega^2[M] + i\omega[B] + [K]$. The forcing vector $\{F\}$ reflects the unit pressure load applied on each panel. Thus, the forcing vector is different when the pressure load is applied on each panel, and the structural vibration is different. In this work it is assumed that the acoustic medium does not affect the structural response; therefore, an uncoupled analysis is performed.

Solving Eq. (1) for $\{u\}$ and multiplying each side of the equation by a transformation matrix $[T]$ produces the normal velocity components on the surface of the acoustic boundary element model:

$$\{v_n\} = [T]\{u\} = [T][St]^{-1}\{F\} \tag{2}$$

The transformation matrix represents a projection of the structural vibration on each element of the acoustic boundary element model. A factor of $(i\omega)$ has been absorbed within $[T]$ to convert displacements into velocities. The vector of normal velocities constitutes the boundary condition for the acoustic analysis. In this work, the direct BEM[4,7,32,33] is utilized for acoustic analysis. The distribution of the unknown acoustic surface pressure $\{p_s\}$ over the boundary element analysis (BEA) model can be computed as

$$[A]\{p_s\} = [B]\{v_n\} = \{f(\{v_n\})\} \tag{3}$$

where $[A]$ and $[B]$ depend on the frequency and the type of BEM analysis and $\{f(\{v_n\})\}$ is the excitation vector that depends on the velocity boundary conditions and matrix $[B]$. After the surface pressure on the BEA model have been computed, the pressure (p_{dr}) at any data recovery location within the acoustic domain can be written as

$$p_{\mathrm{dr}} = \{A_{\mathrm{dr}}\}^T\{p_s\} + \{B_{\mathrm{dr}}\}^T\{v_n\} \tag{4}$$

where vectors $\{A_{\mathrm{dr}}\}$ and $\{B_{\mathrm{dr}}\}$ depend on the geometry, the frequency, and the location of the data recovery point.

Substituting Eqs. (1–3) into Eq. (4) results in

$$p_{\mathrm{dr}} = \{R_{\mathrm{dr}}\}^T\{F\} \tag{5}$$

where $\{R_{\mathrm{dr}}\}^T = \{A_{\mathrm{dr}}\}^T[A]^{-1}[B][T][St]^{-1} + \{B_{\mathrm{dr}}\}^T[T][St]^{-1}$. $\{R_{\mathrm{dr}}\}$ is the complex vector that captures the radiation characteristics within the acoustic medium, the flexural characteristics of the structure, the relative position of the data recovery point, and the frequency of analysis. $\{R_{\mathrm{dr}}\}$ represents a response function between any forcing vector applied on the structure and the acoustic response at a data recovery point. $\{R_{\mathrm{dr}}\}$ must be computed only once for each data recovery point and each frequency of analysis. Multiplying the response function with the forcing vector that originates from a uniform unit pressure load applied on each panel allows the computation of the acoustic pressure at point k due to a unit pressure load at panel i. This acoustic pressure is equal to the transfer function H_{ki}:

$$H_{ki} = p_{\mathrm{dr}_k} = \left\{R_{\mathrm{dr}_k}\right\}^T\{F_i\} \tag{6}$$

H_{ki} is utilized in the stochastic analysis along with the mathematical model of the boundary layer for computing the acoustic response due to the boundary-layer excitation.

The magnitude of the excitation applied on each panel is related with the autospectral terms $S_{F_i F_i}(\omega)$. The degree of correlation between the excitation applied on different panels is expressed by the cross-spectral terms $S_{F_i F_l}(\omega)$. The autospectral density of the radiated acoustic pressure at data recovery point k is computed as

$$S_{p_{\mathrm{dr}_k}}(\omega) = \sum_i \sum_l H_{ki} \cdot H_{kl}^* \cdot S_{F_i F_l}(\omega) \tag{7}$$

Taking into account that the acoustic response at several data recovery points may be required. Equation (7) can be written in matrix form as

$$\left[S_{p_{\mathrm{dr}}}\right] = [H_{\mathrm{dr}}]\left[S_{F_i F_l}\right][H_{\mathrm{dr}}]^H \tag{8}$$

where $[S_{p_{\mathrm{dr}}}]$ is a matrix that contains as diagonal entries the power spectrum of the acoustic pressure at the data recovery points. $[S_{F_i F_l}]$ is the power spectral density of the excitation.

The autospectral density of the acoustic pressure at several data recovery points within the acoustic domain provides a complete description of the radiated sound. The output autospectral density of the acoustic response at a data recovery point can be represented as a sound pressure level (SPL) through the relation

$$\mathrm{SPL}_k = 10 \log\left(\frac{\left|S_{p_{\mathrm{dr}_k}}\right|}{(2 \times 10^{-5}\ \mathrm{Pa})^2}\right) \tag{9}$$

Equation (8) has been utilized for computing the noise radiation from panels that are subjected to boundary-layer excitation. The calculations have been verified by comparison to test data.[26,30]

Radiated Sound Power

Based on the algorithms used for determining the sound pressure spectral density, the radiated sound power for the system can be derived. The radiated sound power can be computed from the surface normal intensity.[34] The normal intensity is defined to be the structural surface pressure multiplied by the normal velocity of the structure. In terms of finite element and boundary element notation, the radiated sound power of a vibrating structure can be expressed in matrix notation as[5]

$$PW = \tfrac{1}{2}\,\mathrm{Re}\left(\{p_s\}^T [Ar]\left\{v_n^*\right\}\right) \tag{10}$$

where $\{p_s\}$ is the vector of elemental surface pressures and $\{v_n^*\}$ is the vector of the conjugate values of the elemental surface normal velocities. Multiplying the velocity vector by the area matrix allows Eq. (10) to be written as

$$PW = \frac{1}{2}\,\mathrm{Re}\left(\{p_s\}^T\left\{va_n^*\right\}\right) = \frac{1}{2}\,\mathrm{Re}\sum_{\mathrm{diag}}\left(\{p_s\}\left\{va_n^*\right\}^T\right) \tag{11}$$

The area modified velocity vector $\{va_n^*\}$ is the result of multiplying the elemental area matrix by the elemental velocity vector. The pressure and velocity vectors in Eq. (11) can be represented in terms of excitation forces and transfer functions as

$$PW = \frac{1}{2}\,\mathrm{Re}\sum_{\mathrm{diag}}\left(E\left[\left[H_{p_s}\right]\{F_i\}\left\{F_l^*\right\}^T\left[H_{va}^*\right]^T\right]\right) \tag{12}$$

where $[H_{p_s}]$ is a matrix of acoustic surface pressure response transfer functions given by Eq. (3) when acoustic surface pressure is computed for each external excitation. $[H_{va}^*]$ is the conjugate matrix of surface velocity transfer functions multiplied by the diagonal area matrix. The surface velocity transfer functions represent the relationship between panel excitation and elemental velocity response. $\{F_i\}$ and $\{F_l^*\}$ are the forcing vectors over each ith panel and the conjugate forcing vector over each lth panel, respectively. The operator E denotes the mean or expected value of a quantity. The surface pressure and surface velocity transfer functions are deterministic; therefore, Eq. (12) can be written as

$$PW = \frac{1}{2}\,\mathrm{Re}\sum_{\mathrm{diag}}\left(\left[H_{p_s}\right]E\left[\{F_i\}\left\{F_l^*\right\}^T\right]\left[H_{va}^*\right]^T\right) \tag{13}$$

By definition, the expected value of the two forcing vectors in Eq. (13) is equal to the spectral density of the excitation applied over the panels. This equality is written as[19]

$$\left[S_{F_i F_l}\right] = E\left[\{F_i\}\left\{F_l^*\right\}^T\right] \tag{14}$$

Substituting Eq. (14) into Eq. (13) results in

$$PW = \frac{1}{2}\,\mathrm{Re}\sum_{\mathrm{diag}}\left(\left[H_{p_s}\right]\left[S_{F_i F_l}\right][H_{va}]^H\right) \tag{15}$$

Equation (15) is the expression utilized for calculating the radiated sound power.

Acoustic Pressure Spectral Density Sensitivity

The sensitivity of the acoustic power spectral density with respect to a given structural design variable is obtained through differentiation of the acoustic power spectral density, Eq. (8), with respect to a structural design variable. Performing this differentiation gives us the following expression for the sensitivity at multiple data recovery locations:

$$\frac{\partial\left[S_{p_{\mathrm{dr}}}\right]}{\partial h_m} = [H_{\mathrm{dr}}]\left[S_{F_i F_l}\right]\frac{\partial[H_{\mathrm{dr}}]^H}{\partial h_m} + \frac{\partial[H_{\mathrm{dr}}]}{\partial h_m}\left[S_{F_i F_l}\right][H_{\mathrm{dr}}]^H \tag{16}$$

where $\partial[H_{\mathrm{dr}}]/\partial h_m$ is the matrix of transfer function sensitivities and $\partial[S_{p_{\mathrm{dr}}}]/\partial h$ contains the sensitivity of the acoustic power spectrum in the diagonal. Matrix $\partial[H_{\mathrm{dr}}]/\partial h_m$ can be written as

$$\frac{\partial[H_{\mathrm{dr}}]}{\partial h_m} = \begin{bmatrix} \frac{\partial H_{11}}{\partial h_m} & \cdots & \frac{\partial H_{1i}}{\partial h_m} & \cdots & \frac{\partial H_{1I}}{\partial h_m} \\ \vdots & & \vdots & & \vdots \\ \frac{\partial H_{k1}}{\partial h_m} & \cdots & \frac{\partial H_{ki}}{\partial h_m} & \cdots & \frac{\partial H_{kI}}{\partial h_m} \\ \vdots & & \vdots & & \vdots \\ \frac{\partial H_{K1}}{\partial h_m} & \cdots & \frac{\partial H_{Ki}}{\partial h_m} & \cdots & \frac{\partial H_{KI}}{\partial h_m} \end{bmatrix} \tag{17}$$

Each structural acoustic component of the sensitivity matrix is obtained by combining structural sensitivities with acoustic sensitivities. According to the chain rule, the matrix components of Eq. (17) can be expressed as

$$\frac{\partial H_{ki}}{\partial h_m} = \left\{\frac{\partial H_k}{\partial v_n}\right\}^T \left\{\frac{\partial v_n}{\partial h_m}\right\}_i \tag{18}$$

where $\{\partial H_k/\partial v_n\}$ is referred to as the acoustic sensitivity vector and represents the sensitivity of the acoustic pressure at the kth data recovery node due to the surface normal velocity. The structural sensitivity vector, $\{\partial v_n/\partial h_m\}_i$, represents the structural sensitivity of the surface normal velocity that is generated from the external excitation applied on the ith panel, due to a change in the structural design variable h_m. The vector $\{\partial H_k/\partial v_n\}$ is independent of the actual velocity boundary conditions, and it is computed only once for each frequency of analysis. The vector $\{\partial v_{ni}/\partial h_m\}$ depends on the excitation applied on the structure and must be computed separately for each load applied on a panel.

When Eqs. (3), (4), and (6) are used, the acoustic sensitivities can be written explicitly as

$$\left\{\frac{\partial H_k}{\partial v_n}\right\} = \left\{\{A_{\mathrm{dr}}\}^T[A]^{-1}[B] + \{B_{\mathrm{dr}}\}^T\right\} \tag{19}$$

The right-hand side of Eq. (19) comprises matrices and vectors that are calculated when determining the acoustic pressure spectral density. Therefore, no additional computations are required for calculating the acoustic sensitivities.

The structural sensitivities are obtained by differentiating Eq. (2):

$$\left\{\frac{\partial v_n}{\partial h_m}\right\}_i = [T]\left\{\frac{\partial u}{\partial h_m}\right\}_i \tag{20}$$

where $\{u\}_i$ = vector of displacements created on the structure due to application of uniform pressure on the ith panel. The sensitivity of the nodal displacements is computed[35]:

$$\left\{\frac{\partial u}{\partial h_m}\right\}_i = -[-\omega^2[M] + i\omega[B] + [K]]^{-1} \times \left[-\omega^2\frac{\partial[M]}{\partial h_m} + i\omega\frac{\partial[B]}{\partial h_m} + \frac{\partial[K]}{\partial h_m}\right]\{u\}_i \tag{21}$$

Because the value of $\{u\}_i$ appears on the right-hand side of Eq. (21), the structural sensitivity $\{\partial u/\partial h_m\}_i$ depends on the vibration and, therefore, on the applied structural load. Thus, $\{\partial u/\partial h_m\}_i$ must be computed separately for the external load applied on each panel. Once the structural sensitivities and the acoustic sensitivities have been calculated for a given frequency, they are inserted into Eq. (18) and the structural/acoustic sensitivities are determined. Then, the matrix multiplication expressed in Eq. (16) is performed to obtain the sensitivity of the acoustic pressure density with respect to design variable h_m.

Radiated Sound Power Sensitivity

The sensitivity of the radiated sound power is calculated by differentiating Eq. (15) with respect to a structural design variable:

$$\frac{\partial PW}{\partial h_m} = \sum_{\text{diag}}\frac{1}{2}\,\text{Re}\left(\left[H_{ps}\right]\left[S_{F_i F_l}\right]\frac{\partial[H_{va}]^H}{\partial h_m} + \frac{\partial\left[H_{ps}\right]}{\partial h_m}\left[S_{F_i F_l}\right][H_{va}]^H\right) \tag{22}$$

where $\partial[H_{va}]^H/\partial h_m$ is the Hermitian transpose of the structural sensitivities and has dimensions equal to the number of panels by number of elements in the model and $\partial[H_{ps}]/\partial h_m$ is the matrix of the structural/acoustic sensitivities for the acoustic surface pressure and has dimensions equal to the number of elements by number of panels. In the computation of the power sensitivity, the columns of the structural sensitivity matrix, $\partial[H_{va}]/\partial h_m$, are obtained by multiplying Eq. (20) by the diagonal area matrix $[Ar]$ for each panel. The computation of $\partial[H_{ps}]/\partial h_m$ is performed by evaluating the acoustic sensitivity of the acoustic surface pressure and combining it with the structural sensitivity. The acoustic sensitivity of the acoustic surface pressure can be computed by differentiating Eq. (3) with respect to the normal velocity of each element:

$$\left[\frac{\partial p_s}{\partial v_n}\right] = [A]^{-1}[B] \tag{23}$$

where $[\partial p_s/\partial v_n]$ contains in each column the derivative of all of the acoustic surface pressures with respect to the normal velocity of a particular element. Each column corresponds to a differentiation with respect to a different element velocity. The structural/acoustic sensitivity of the acoustic surface pressure is computed as

$$\frac{\partial\left[H_{ps}\right]}{\partial h_m} = \left[\frac{\partial p_s}{\partial v_n}\right]\frac{\partial[H_v]}{\partial h_m} \tag{24}$$

where $\partial[H_v]/\partial h_m$ contains as columns the structural sensitivities $\{\partial v_{ni}/\partial h_m\}$ that are computed by Eq. (20). Then, the sensitivity of the radiated power with respect to a structural design variable is computed from Eq. (22).

Application and Validation of Results

Two plate configurations are analyzed to validate the developed algorithms and to demonstrate their functionality. A simply supported flat plate and a stiffened simply supported plate are considered. The fluctuating pressure of boundary-layer flow comprises the excitation and is applied on one side of the plate while the acoustic radiation from the opposite side in a free field is computed. The dimensions and the properties of the flat plate are identical to a configuration that has been analyzed in the past[26] and correlated with the test data available in the literature.[36] The stiffened plate is derived from the flat plate by adding transverse stiffeners to the radiating side. The stiffeners are only added to the structural model because the effect of the stiffeners as noise sources is considered negligible.

Structural/acoustic analyses are performed for baseline designs of the two configurations in the frequency range 50–1000 Hz. The sound pressure spectral density is computed at three data recovery nodes. One of the data recovery nodes is positioned along the centerline of the plate and the other two at symmetric positions with respect to the centerline to inspect the calculations for the expected symmetry. The radiated sound power is computed at four frequencies that demonstrate consistently high values for the acoustic pressure response at the three data recovery points. Sensitivity computations for the sound pressure spectral density and the radiated sound power are performed at frequencies bracketing the four frequencies of peak response. The computed structural/acoustic sensitivities are compared to values derived from finite difference analyses. Good correlation is observed for both the pressure spectral density and the radiated power.

To perform the computations associated with the theoretical developments presented in the preceding section, a commercial FEM code and the software implementation of the acoustic and the sensitivity computations are utilized. A commercial FEM code is used for calculating the structural matrices, the excitation vectors, and the structural sensitivity of a structure that is subjected to unit external load applied on each panel subdivision.

New software has been developed for computing 1) the noise radiated from the structural vibration, 2) the acoustic sensitivity of the acoustic pressure at a data recovery point or on the surface of the BEM model with respect to the velocity boundary conditions, 3) the radiated noise and radiated power from a structure subjected to stochastic excitation, and 4) the structural/acoustic sensitivity of the radiated noise and the radiated acoustic power when the structure is subjected to stochastic excitation.

The direct BEM is utilized for performing computations 1 and 2. The structural vibration, the structural sensitivity, the acoustic results, and the acoustic sensitivity are combined along with the stochastic definition of the excitation in computations 3 and 4 for performing the computations outlined.

The stochastic excitation employed in the applications corresponds to the fluctuating pressure of a turbulent boundary-layer airflow over a flat surface. The autospectral density of the pressure distribution is typical of a 35.8 m/s boundary-layer flow.[26,36] The autospectral density of the excitation generates the diagonal terms of $[S_{F_i F_l}]$. The off-diagonal values, cross-spectrum terms, of the excitation matrix are generated using the semi-empirical equations provided by Smol'yakov and Tkachenko.[24] The cross-spectral density terms are a function of frequency, panel separation, autospectral density value, flow speed, and turbulent boundary-layer thickness. Details regarding the description of the excitation matrix are presented in Refs. 24 and 26.

Simply Supported Plate

The first structure analyzed is a simply supported flat plate. The plate is made of aluminum with the characteristics described in Table 1. The finite element model of this structure consists of 270 nodes and 238 quadrilateral elements. This descritization is selected to represent adequately the highest anticipated mode of vibration in the frequency range of analysis. Analysis of this structural acoustic system is conducted over the frequency range 0–1000 Hz. The finite element model is shown in Fig. 1. The origin is placed at the lower left corner of the model as shown in Fig. 1. The simply supported plate lies on the $z = 0$ plane. The turbulent boundary-layer flow excitation is distributed over the entire $+z$ face of the plate. Figure 1 also shows the panel division used in this analysis. A division of 30 panels was found to capture accurately the effects of the excitation.[26] The FEM model is utilized for generating the structural matrices and the forcing vectors. During the sensitivity analysis, it is utilized for computing the structural sensitivities.

Sound pressure density values are calculated at three data recovery nodes. All three data recovery nodes are located at the end of the plate farthest downstream. One data recovery node (DR node 2) is placed at the centerline of the plate, while the other two (DR nodes 1 and 3) are placed at the opposing plate corners symmetric to the centerline. The thickness of the plate is utilized for defining the structural design variables. Two separate plate thickness configurations are analyzed. In both configurations, the plate is divided into thickness strips aligned with one of the principle axes of the plate. The first configuration consists of four strips positioned longitudinally. The thickness of the plate at each strip is considered as an independent design variable. The second configuration consists of five strips running transversely along the plate, and the corresponding plate thicknesses of the strip constitute the design variables. A uniform thickness distribution is considered as the baseline design for all sensitivity computations. The initial thickness for the design variables is listed in Table 1. The two thickness configurations for the simply supported plate are shown in Fig. 2 along with the three DR nodes. DR nodes 1, 2, and 3 are located at (0.458, −0.035, 0.458) m, (0.458, 0.165, 0.458) m, and (0.458, 0.365, 0.458) m, respectively. All distances are referenced to the origin in Fig. 1. The three DR nodes used in this analysis lie approximately one plate length in front of the vibrating surface.

Sound is considered to radiate from the side of the vibrating plate opposite to the side where the boundary-layer excitation is applied. Therefore, the boundary element model consists of a flat section representing the radiating side of the flexible plate and a cover composed of five rigid sides attached to the flexible plate.[26] The presence of the rigid cover in the acoustic model is necessary to permit noise radiation only from one side of the flexible plate. The boundary element model consists of 664 nodes and 1324 triangular elements. The depth of the cover is 0.08 m. The depth value is selected to ensure that no irregular frequencies will be encountered during solution of the BEM system of equations, and it does not affect the SPLs calculated in the numerical analysis. The presence of the cover suppresses the noise radiated from the enclosed side of the plate.

A baseline acoustic pressure spectral density curve is generated for DR node 1. Figure 3 shows the results of 50 analyzed frequencies. In Fig. 3, the acoustic pressure spectral density is presented in terms of its equivalent decibel value calculated from Eq. (9). The frequencies of analysis that define the curve in Fig. 3 are selected such that the system resonances would be accurately represented. The first two system resonances occur at 165 and 333 Hz. These frequencies coincide with the first normal mode (1,1) and the second normal mode (2,1) calculated from the analytical solution of a simply supported plate. Correlation of the baseline results presented in Fig. 3 with test data has been presented in Ref. 26. The baseline

Table 1 Characteristics for the simply supported plate and stiffened simply supported plate

Characteristic	Value
Material	Aluminum
Density	2.7×10^3 kg/m^3
Poisson's ratio	0.33
Young's modulus	7.3×10^{10} N/m^2
Length	0.46 m
Width	0.33 m
Initial thickness	0.0048 m
Structural damping	2.0%
Stiffener length	0.33 m
Flange width	0.0271 m
Web height	0.0361 m
Stiffener initial thickness	0.0048 m

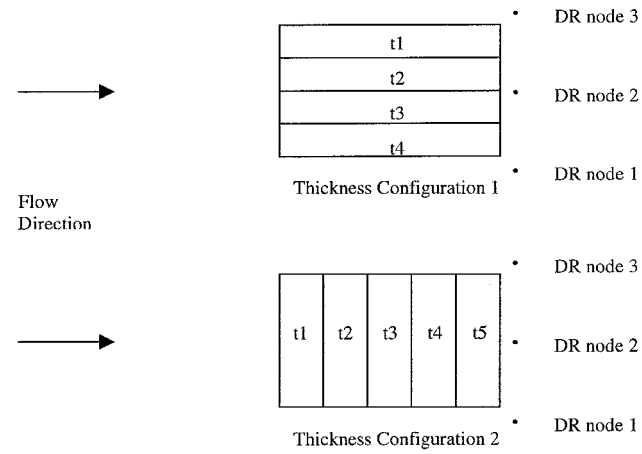

Fig. 2 Thickness configurations for the simply support plate and DR node locations.

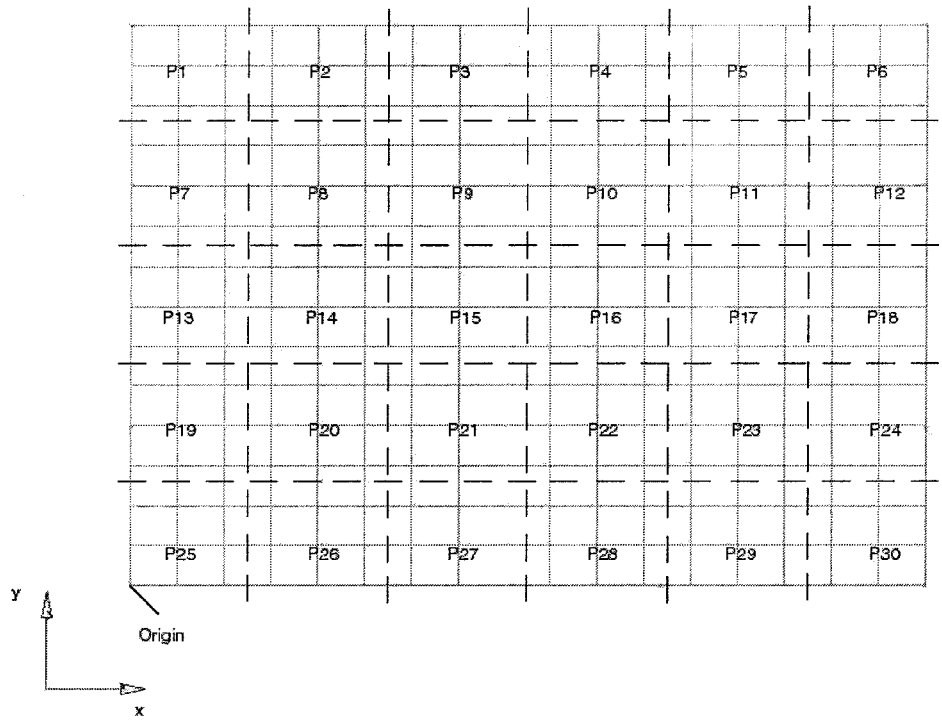

Fig. 1 Simply supported plate finite element model, panel configuration, and reference origin.

Table 2 SPL results with associated acoustic PSD values for frequencies bracketing first two structural resonances of the simply supported plate

Frequency, Hz	DR node 1		DR node 2		DR node 3	
	SPL, dB	PSD, Pa^2/Hz	SPL, dB	PSD, Pa^2/Hz	SPL, dB	PSD, Pa^2/Hz
163.0	43.4	$8.69E-06$	44.2	$1.05E-05$	43.4	$8.69E-06$
167.0	45.1	$1.29E-05$	45.9	$1.56E-05$	45.1	$1.29E-05$
331.0	37.9	$2.47E-06$	39.4	$3.45E-06$	37.9	$2.47E-06$
335.0	36.2	$1.68E-06$	37.6	$2.33E-06$	36.2	$1.68E-06$

Table 3 Sensitivity values for the acoustic PSD with respect to configuration 1 design variables

Frequency, Hz	Acoustic PSD sensitivity, $Pa^2/m \cdot Hz$[a]			
	$t1$	$t2$	$t3$	$t4$
163.0	$-5.68E-02$	$-5.06E-02$	$-5.06E-02$	$-5.68E-02$
167.0	$8.38E-02$	$7.18E-02$	$7.18E-02$	$8.38E-02$
331.0	$-1.18E-02$	$-1.09E-02$	$-1.09E-02$	$-1.18E-02$
335.0	$1.11E-02$	$9.74E-02$	$9.74E-02$	$1.11E-02$

[a]Results for DR node 2.

Table 4 Sensitivity values for the acoustic PSD with respect to configuration 2 design variables

Frequency, Hz	Acoustic PSD sensitivity, $Pa^2/m \cdot Hz$[a]				
	$t1$	$t2$	$t3$	$t4$	$t5$
163.0	$-3.79E-02$	$-3.31E-02$	$-3.53E-02$	$-3.33E-02$	$-3.82E-02$
167.0	$5.65E-02$	$4.76E-02$	$4.99E-02$	$4.74E-02$	$5.61E-02$
331.0	$-7.90E-03$	$-6.05E-03$	$-4.95E-03$	$-6.31E-03$	$-7.45E-023$
335.0	$6.74E-03$	$5.71E-03$	$4.73E-03$	$5.53E-03$	$7.01E-03$

[a]Results for DR nodes 1 and 3.

Table 5 Radiated sound power and sound power sensitivity values with respect to thickness configuration 1 design variables

Frequency, Hz	Radiated sound power, N · m/s	Sound power sensitivity, N/s			
		$t1$	$t2$	$t3$	$t4$
163.0	$2.98E-08$	$-1.81E-04$	$-1.60E-04$	$-1.61E-04$	$-1.82E-04$
167.0	$4.46E-08$	$2.36E-04$	$2.02E-04$	$2.02E-04$	$2.35E-04$
331.0	$1.18E-08$	$-4.20E-05$	$-3.86E-05$	$-3.86E-05$	$-4.20E-05$
335.0	$7.11E-09$	$3.50E-05$	$3.08E-05$	$3.08E-05$	$3.50E-05$

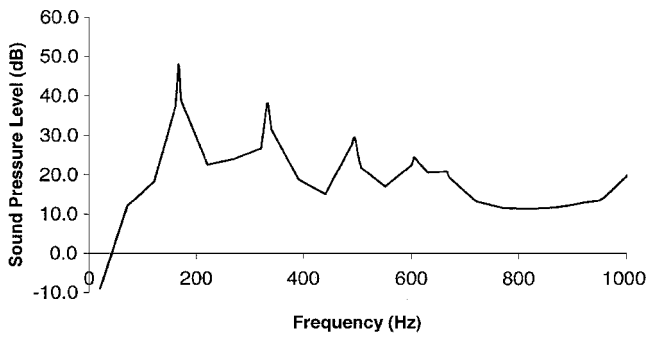

Fig. 3 Baseline SPL response for the simply supported plate at DR node 1.

response curve is generated for DR node 1, an off-axis location, so that all of the system resonances will appear. From Fig. 3, 20 frequencies are selected at which the sensitivity analysis is performed. The expected symmetry is observed in the acoustic results between positions of DR node 1 and DR node 3. For brevity, results for only the four frequencies surrounding the first two resonances are presented (Table 2). Because of the symmetry of the structural/acoustic system, the acoustic pressure results for the two data recovery nodes along the plate corners (DR nodes 1 and 3) are the same.

The sensitivity of the acoustic pressure spectral density is calculated for the four frequencies listed in Table 2. Sensitivity values are calculated with respect to the structural design variables defined in the two thickness configurations considered in this work. Table 3 contains the acoustic pressure spectral density sensitivities for the four thickness design variables corresponding to the design variables of configuration 1. The sensitivity values are provided for DR node 2. Because of symmetry, the sensitivity values with respect to design variables $t1$ and $t4$, as well as $t2$ and $t3$, are expected to be the same. The symmetry criterion is satisfied according to the results presented in Table 3. The sensitivity values calculated for DR nodes 1 and 3 with respect to the five design variables of configuration 2 are expected to be the same. The sensitivities are listed in Table 4. Sensitivity values calculated for DR nodes 1 and 3 are the same, as anticipated. Sensitivity calculations for each configuration took approximately 6.0×10^3 CPU seconds per frequency of analysis.

The radiated sound power and the radiated sound power structural/acoustic sensitivity are calculated at the same four frequencies for configuration 1 and are listed in Table 5. Sensitivity computations took approximately 1.3×10^4 CPU seconds per frequency. Similar to the sound pressure spectral density values for this configuration, the sound power sensitivities display the appropriate symmetry with respect to the symmetric design variables.

To further validate the sensitivity computations, certain design variables are altered and reanalysis is performed. Acoustic pressure spectral density and sound power values are computed for the modified designs. The new acoustic pressure spectral density and sound power values are compared to expected values that are predicted from the sensitivity computations as

$$Q(\omega) = Q_i(\omega) + \sum_{m=1}^{n} \frac{\partial Q(\omega)}{\partial h_m} \cdot \Delta_m \tag{25}$$

$Q(\omega)$ is either the sound power spectral density at a DR node or the radiated sound power. $Q_i(\omega)$ is the value of the quantity of interest for the baseline design, $\partial Q(\omega)/\partial h_m$ is the structural/acoustic sensitivity of the quantity of interest with respect to structural design variable h_m, Δ_m is the change in the structural design variable h_m, and n is the number of structural design values perturbed. For configuration 1, design variable $t4$ is increased by 3%. The sound power spectral density at DR node 2 and the radiated sound power are predicted according to Eq. (25). The results are compared to the actual values computed for the modified design (Table 6). Good agreement exists between the values predicted from the utilization of the structural/acoustic sensitivities and the reanalysis results with the exception of results at 163.0 Hz. Sensitivity calculations at this particular frequency represent a response shift into the very sharp first structural resonance of 165 Hz. Therefore, because Eq. (25) constitutes a linear approximation, it cannot capture accurately the occurring change when moving in an extremely narrow resonance peak. Similar computations are performed for configuration 2 and a 3% increase in the thickness of design variable $t5$. Results for the acoustic pressure spectral density at DR node 2 are summarized in Table 7, and good correlation is observed.

Stiffened Simply Supported Plate

The second structure analyzed is a stiffened, simply supported plate. This structure is derived from the simply supported plate described in the preceding section by adding two L-shaped transverse stiffeners equidistant along the length of the plate. The stiffened, simply supported plate is analyzed as a representative configuration of an aerospace application that constitutes a geometrically more complex structure than the simply supported plate. The turbulent boundary-layer flow is considered to apply excitation on the smooth side of the stiffened plate. Acoustic radiation is considered from the stiffened side of the plate into an unbounded acoustic medium. The stiffeners are assumed not to have any source effects or impact the directivity of the radiated sound.

Table 6 Finite difference results vs actual reanalysis results of acoustic response quantities[a]

Frequency, Hz	Acoustic PSD, Pa^2/Hz[b]		Radiated sound power, N · m/s	
	Predicted	Actual	Predicted	Actual
163.0	3.71E−06	5.25E−06	3.59E−09	1.31E−08
167.0	2.56E−05	2.95E−05	7.84E−08	7.37E−08
331.0	2.22E−06	1.64E−06	5.76E−09	5.89E−09
335.0	3.46E−06	3.83E−06	1.22E−08	1.25E−08

[a]Change in design variable $t4$, thickness configuration 1. [b]Results for DR node 2.

Table 7 Finite difference results vs actual reanalysis results of acoustic PSD[a]

Frequency, Hz	Acoustic PSD, Pa^2/Hz[b]	
	Predicted	Actual
163.0	3.85E−06	5.88E−06
167.0	2.54E−05	2.73E−05
331.0	1.96E−06	1.84E−06
335.0	3.74E−06	3.73E−06

[a]Change in design variable $t5$, thickness configuration 2.
[b]Results for DR node 2.

The finite element model for the stiffened simply supported plate appears in Fig. 4. The characteristics of the stiffeners are listed in Table 1. The simply supported plate, also described in Table 1, forms the base to which the stiffeners are attached. The finite element model for the stiffened, simply supported plate comprises of 561 nodes and 378 quadrilateral elements. The structural design variables for the stiffened plate comprise the four thickness variables associated with configuration 1 of the flat plate, plus eight additional design variables associated with the thickness of the stiffeners. The eight additional structural design variables associated with the stiffeners are shown in Fig. 4. The natural frequencies of the stiffened plate are calculated via modal analysis and used as a basis for selecting frequencies of analysis.

Similar to the simply supported plate, the acoustic pressure spectral density baseline response curve is generated for DR node 1 over the 1000-Hz frequency range. The results are shown in Fig. 5. As expected, because of the inclusion of stiffeners, resonances appear at higher frequencies. The two highest acoustic pressure spectral density levels occur at frequencies of 635 and 685 Hz. Four frequencies bracketing the two peak responses are selected for further sensitivity analysis. Values for the sound pressure spectral density at the three data recovery nodes are given in Table 8. Once again the acoustic results at DR nodes 1 and 3 display symmetry as expected.

Sensitivity values for the acoustic pressure spectral density (PSD) at DR node 2 are calculated with respect to all 12 design variables detailed in Figs. 2 and 4. These sensitivities are listed in Table 9. The structural/acoustic sensitivity results with respect to symmetrically placed design variables acquire the same values as expected. The acoustic pressure sensitivity calculations took approximately 8.0×10^3 CPU seconds per frequency of analysis to complete. The radiated sound power and the structural/acoustic sensitivity of the sound power are calculated with respect to all 12 stiffener design variables, and results are summarized in Table 10. The sound power sensitivity calculations required 1.4×10^4 CPU seconds per frequency. The results reflect all expected equality trends due to the symmetry demonstrated in the definition of the structural design variables.

To further validate the structural/acoustic sensitivity, computations for the stiffened plate perturbations are introduced in the design

Table 8 SPLs with associated acoustic PSD value for frequencies bracketing the first two structural resonances of the stiffened, simply supported plate

Frequency, Hz	DR node 1		DR node 2		DR node 3	
	SPL, dB	PSD, Pa^2/Hz	SPL, dB	PSD, Pa^2/Hz	SPL, dB	PSD, Pa^2/Hz
628.0	39.0	3.20E−06	40.5	4.44E−06	39.0	3.20E−06
637.0	39.0	3.21E−06	40.5	4.49E−06	39.0	3.21E−06
683.0	38.2	2.67E−06	39.3	3.39E−06	38.2	2.67E−06
687.0	39.0	3.20E−06	40.1	4.07E−06	39.0	3.20E−06

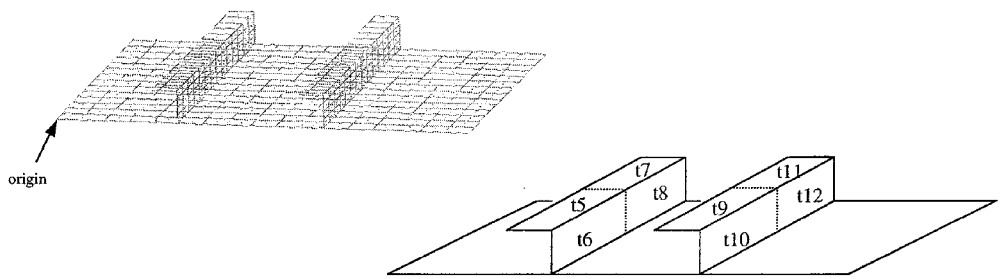

Fig. 4 Finite element model of the stiffened, simply supported plate and design variable definition.

Table 9 Sensitivity values for the acoustic PSD with respect to 12 design variables of the stiffened, simply supported plate[a]

Frequency, Hz	Acoustic PSD sensitivity, $Pa^2/m \cdot Hz$[a]											
	$t1$	$t2$	$t3$	$t4$	$t5$	$t6$	$t7$	$t8$	$t9$	$t10$	$t11$	$t12$
628.0	$-1.12E-02$	$-1.21E-02$	$-1.21E-02$	$-1.12E-02$	$1.20E-03$	$-1.31E-03$	$1.20E-03$	$-1.31E-03$	$-2.07E-03$	$-5.36E-03$	$-2.07E-03$	$-5.36E-03$
637.0	$1.21E-02$	$1.28E-02$	$1.28E-02$	$1.21E-02$	$-2.01E-03$	$2.21E-03$	$-2.01E-03$	$2.21E-03$	$1.55E-03$	$4.27E-03$	$1.55E-03$	$4.27E-03$
683.0	$-4.28E-03$	$-6.07E-03$	$-6.07E-03$	$-4.28E-03$	$9.00E-06$	$-5.28E-03$	$9.00E-06$	$-5.28E-03$	$-6.22E-05$	$-7.72E-04$	$-6.22E-05$	$-7.72E-04$
687.0	$9.15E-05$	$-6.42E-05$	$-6.42E-05$	$9.15E-05$	$1.05E-04$	$6.93E-04$	$1.05E-04$	$6.93E-04$	$1.32E-04$	$7.74E-04$	$1.32E-04$	$7.74E-04$

[a]Results for DR node 2.

Table 10 Sound power and sound power sensitivity values with respect to 12 design variables of the stiffened, simply supported plate[a]

Frequency, Hz	Sound power, $N \cdot m/s$	Sound power sensitivity, N/s											
		$t1$	$t2$	$t3$	$t4$	$t5$	$t6$	$t7$	$t8$	$t9$	$t10$	$t11$	$t12$
628.0	$1.20E-09$	$-3.11E-06$	$-3.36E-02$	$-3.36E-02$	$-3.11E-06$	$3.47E-07$	$-3.68E-07$	$3.47E-07$	$-3.68E-07$	$-5.65E-07$	$-1.46E-06$	$-5.65E-07$	$-1.46E-06$
637.0	$1.21E-09$	$3.14E-06$	$3.30E-06$	$3.30E-06$	$3.14E-06$	$-5.14E-07$	$5.76E-07$	$-5.14E-07$	$5.76E-07$	$4.08E-07$	$1.13E-06$	$4.08E-07$	$1.13E-06$
683.0	$7.96E-10$	$-9.67E-07$	$-1.38E-06$	$-1.38E-06$	$-9.67E-07$	$-9.95E-09$	$-1.19E-06$	$-9.91E-09$	$-1.19E-06$	$-2.23E-08$	$-1.89E-07$	$-2.23E-08$	$-1.89E-07$
687.0	$9.45E-10$	$5.76E-08$	$3.12E-08$	$3.13E-08$	$5.77E-08$	$1.10E-08$	$2.15E-07$	$1.11E-08$	$2.15E-07$	$2.16E-08$	$1.69E-07$	$2.16E-08$	$1.69E-07$

[a]Results for DR node 2.

Table 11 Finite difference results vs actual reanalysis results of acoustic response quantities[a]

Frequency, Hz	Acoustic PSD, Pa^2/Hz[b]		Radiated sound power, N · m/s	
	Predicted	Actual	Predicted	Actual
628.0	2.43E−06	2.52E−06	9.03E−10	9.43E−10
637.0	3.80E−06	3.76E−06	1.43E−09	1.41E−09
683.0	2.57E−06	2.57E−06	7.66E−10	7.65E−10
687.0	3.30E−06	3.29E−06	9.72E−10	9.68E−10

[a]Uniform increase in design variables $t9$ and $t10$, stiffened simply supported plate.
[b]Acoustic pressure results for DR node 2.

Table 12 Finite difference results vs actual reanalysis results of acoustic PSD[a]

Frequency, Hz	Acoustic PSD, Pa^2/Hz[b]	
	Predicted	Actual
628.0	2.68E−06	2.72E−06
637.0	3.60E−06	3.59E−06
683.0	2.60E−06	2.60E−06
687.0	3.27E−06	3.26E−06

[a]Uniform increase in design variables $t9$–$t12$, stiffened simply supported plate.
[b]Results for DR node 2.

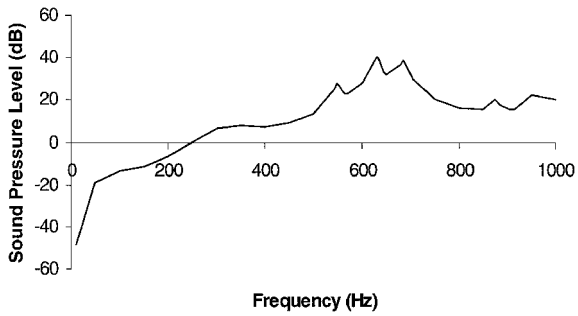

Fig. 5 SPL of corresponding sound PSD for the stiffened simply supported plate: results at DR node 1.

variables and reanalyses are performed. First, the thickness associated with structural design variables $t9$ and $t10$ are increased by 3%. The spectral density of the acoustic pressure and the radiated power are computed from the structural/acoustic sensitivities and the baseline response according to Eq. (25). The same acoustic variables are computed through reanalysis of the perturbed design. The results are summarized in Table 11, and good correlation is observed between the predicted and actual values. Then, a uniform increase of 1% is imposed to all of the design variables $t9$–$t12$, and similar computations are performed for the spectral density of the acoustic pressure at DR node 2. The results are summarized in Table 12, and good correlation is observed.

Conclusions

New algorithms for calculating the radiated sound power and the structural/acoustic sensitivities of a structure subject to stochastic excitation are presented. To validate and demonstrate the new developments, sensitivity analyses are conducted for two models. The fluctuating wall pressure of a turbulent boundary layer provides the stochastic excitation in the two applications. The first configuration is a simply supported flat plate that has been utilized in previous structural/acoustic studies. The second structure is a stiffened simply supported plate. The fluctuating pressure of a boundary layer is applied on one side of the plates. Acoustic radiation from the opposite side is considered. The sensitivity of the acoustic response with respect to a set of structural design values for both models are calculated and validated through comparison with reanalysis results. Expected trends due to symmetry in the definition of the design variables are also observed in the results. The structural/acoustic sensitivity algorithms presented in this paper extend sensitivity analysis techniques to structural/acoustic systems subjected to stochastic excitation.

Acknowledgments

The authors would like to thank the University of Michigan, Rackham School of Graduate Studies, and the U.S. Department of Defense for providing the funding for this project.

References

[1]Bathe, K. J., *Finite Element Procedures in Engineering Analysis*, Prentice–Hall, Englewood Cliffs, NJ, 1982.
[2]Huebner, K. H., and Thornton, E. A., *The Finite Element Method for Engineers*, 2nd ed., Wiley, New York, 1982.
[3]Callister, J. R., and George, A. R., "The Transmission of Aerodynamically-Generated Noise Through Panes in Automobiles," *Second International Congress on Recent Developments in Air- and Structure-Borne Sound and Vibration*, International Inst. of Acoustics and Vibration, Auburn Univ., Auburn, AL, 1992, pp. 1535–1542.
[4]Chertock, G., "Sound Radiation from Vibrating Surfaces." *Journal of the Acoustical Society of America*, Vol. 36, No. 7, 1964, pp. 1305–1313.
[5]Ciskowski, R. D., and Brebbia, C. A., *Boundary Elements in Acoustics*, Elsevier Applied Science, New York, 1991, Chap. 4.
[6]Cunefare, K. A., and Koopmann, G., "A Boundary Element Method for Acoustic Radiation Valid for All Wave Numbers," *Journal of the Acoustical Society of America*, Vol. 85, No. 1, 1989, pp. 39–47.
[7]Koopman, G. H., and Benner, H., "Method for Computing the Sound Power of Machines Based on the Helmholtz Integral." *Journal of the Acoustical Society of America*, Vol. 71, No. 1, 1982, pp. 77–89.
[8]Choi, K. K., Shim, I., and Wang, S., "Design Sensitivity Analysis of Structure-Induced Noise and Vibration." *Journal of Vibration and Acoustics*, Vol. 119, No. 2, 1997, pp. 173–179.
[9]Cunefare, K. A., and Koopmann, G. H., "Acoustic Design Sensitivity for Structural Radiators," *Transactions of the American Society of Mechanical Engineers*, Vol. 114, No. 2, 1992, pp. 178–186.
[10]Hambric, S. A., "Sensitivity Calculations for Broad-Band Acoustic Radiated Noise Design Optimization Problems," *Journal of Vibration and Acoustics*, Vol. 118, No. 3, 1996, pp. 529–532.
[11]Salagame, R. R., Belegundu, A. D., and Koopmann, G. H., "Analytical Sensitivity of Acoustic Power Radiated from Plates," *Journal of Vibration and Acoustics*, Vol. 117, No. 1, 1995, pp. 43–48.
[12]Vlahopoulos, N., Dagg, C., and Bernhard, R. J., "Computation of Sensitivities for Passive Noise Control," *Proceedings NOISECON93*, Inst. of Noise Control Engineering, Saddle River, NJ, 1993, pp. 529–534.
[13]Vlahopoulos, N., Raveendra, S. T., and Mollo, C., "Acoustic Sensitivity Analysis using Boundary Elements and Structural Dynamic Response," MSC 1994 User's Conf., MacNeal–Schwendler Corp., Los Angeles, Paper 7, June 1994.
[14]Bhat, W. V., and Wilby, J. F., "Interior Noise Radiated by an Airplane Fuselage Subjected to Turbulent Boundary Layer Excitation and Evaluation of Noise Reduction Treatments," *Journal of Sound and Vibration*, Vol. 18, No. 4, 1971, pp. 449–464.
[15]Mathur, G. P., and Chin, C. L., "Sound Transmission through Stiffened Aircraft Structures," *Proceedings of NOISECON96*, Inst. of Noise Control Engineering, Saddle River, NJ, 1996, pp. 199–204.
[16]Mixson, J. S., and Wilby, J. F., "Chapter 16. Interior Noise" *Aeroacoustics of Flight Vehicles, Vol. 2, Noise Control*, edited by H. H. Hubbard, Acoustical Society of America, Sewickley, PA, 1995.
[17]Keiji, S., and Toyoki, S., "Research on Aerodynamic Noise around Automobiles," *Society of Automotive Engineers of Japan Review*, Vol. 16, No. 2, 1995, pp. 157–164.
[18]Watanabe, M., Harita, M., and Hayashi, E., "The Effect of Body Shapes on Wind Noise," Society of Automotive Engineers, SAE Paper 780268, 1978.
[19]Wu, S. F., Wu, G., Puskarz, M. M., and Gleason, M. E., "Noise Transmission through a Vehicle Side Window due to Turbulent Boundary Layer Excitation," *Journal of Vibration and Acoustics*, Vol. 119, No. 4, 1997, pp. 557–562.
[20]Davies, H. G., "Low Frequency Random Excitation of Water-Loaded Rectangular Plates," *Journal of Sound and Vibration*, Vol. 15, No. 1, 1971, pp. 107–126.
[21]Bhat, W. V., "Flight Test Measurement of Exterior Turbulent Boundary Layer Pressure Fluctuations on Boeing 737 Airplane," *Journal of Sound and Vibration*, Vol. 14, No. 4, 1971, pp. 439–457.
[22]Howe, M. S., "Surface Pressures and Sound Produced by Turbulent Flow over Smooth and Rough Walls," *Journal of the Acoustical Society of America*, Vol. 90, No. 2, 1991, pp. 1041–1047.
[23]Mathur, G. P., Chin, C. L., and Simpson, M. A., "Transmission Loss of a Panel Excited by Turbulent Boundary Layer Pressure Field," *Proceedings of NOISECON96*, Inst. of Noise Control Engineering, Saddle River, NJ, 1996, pp. 205–210.
[24]Smol'yakov, A. V., and Tkachenko, V. M., "Model of a Field of Pseudosonic Turbulent Wall Pressures and Experimental Data," *Soviet Physical Acoustics*, Vol. 37, No. 6, 1991, pp. 627–631.

[25] Vaicatis, R., Jan, C. M., and Shinozuka, M., "Nonlinear Panel Response from a Turbulent Boundary Layer," *AIAA Journal*, Vol. 10, No. 7, 1972, pp. 895–900.

[26] Allen, M. J., and Vlahopoulos, N., "Integration of Finite Element and Boundary Element Methods for Calculating the Radiated Sound from a Randomly Excited Structure," *Computers and Structures*, Vol. 77, No. 2, 2000, pp. 155–169.

[27] Huntington, D. E., and Lyrintzis, C. S., "Noise Transmission of Skin-Stringer Panels Using a Decaying Wave Method," *AIAA Journal*, Vol. 31, No. 7, 1993, pp. 1338–1340.

[28] Lyrintzis, C. S., and Vaicatis, R., "Random Response and Noise Transmission of Discretely Stiffened Composite Panels," *Journal of Aircraft*, Vol. 27, No. 2, 1989, pp. 176–184.

[29] Vaicatis, R., and Slazak, M., "Noise Transmission through Stiffened Panels," *Journal of Sound and Vibration*, Vol. 70, No. 3, 1980, pp. 413–426.

[30] Allen, M. J., and Vlahopoulos, N., "Noise Generated from a Flexible and Elastically Supported Structure Subject to Turbulent Boundary Layer Flow Excitation," *Finite Elements in Analysis and Design* (to be published).

[31] Gockel, M. A. (ed.), *MSC/NASTRAN Handbook for Dynamic Analysis*, Ver. 63, MacNeal–Schwendler Corp., Los Angeles, 1983.

[32] Seybert, A. F., Soenarko, B., Rizzo, F. J., and Shippy, D. J., "Application of the BIE Method to Sound Radiation Problems Using an Isoparametric Element," *Journal of Vibration, Acoustics, Stress, and Reliability in Design*, Vol. 106, No. 3, 1984, pp. 414–419.

[33] Seybert, A. F., Soenarko, B., Rizzo, F. J., and Shippy, D. J., "An Advanced Computational Method for Radiation and Scattering of Acoustic Waves in Three Dimensions," *Journal of the Acoustical Society of America*, Vol. 77, No. 2, 1985, pp. 362–386.

[34] Pierce, A. D., *Acoustics; An Introduction to Its Physical Principals and Applications*, McGraw–Hill (published through the Acoustical Society of America), New York, 1991, pp. 38, 39, 66–70.

[35] *Seminar Notes, Design Sensitivity and Optimization in MSC/NASTRAN*, MacNeal–Schwendler Corp., Los Angeles, 1993.

[36] Heatwole, C. M., Franchek, M. A., and Bernhard, R. J., "A Robust Feedback Controller Implementation for Flow Induced Structural Radiation of Sound," *Proceedings of NOISECON96*, Inst. of Noise Control Engineering, Saddle River, NJ, 1996, pp. 357–362.

P. J. Morris
Associate Editor